

# Monochromator-induced glitches in EXAFS data

## I. Test of the model for linearly tapered samples

F. Bridges, G.G. Li and Xun Wang

*University of California, Santa Cruz, CA 95064, USA*

Received 24 October 1991 and in revised form 16 March 1992

When EXAFS samples are slightly nonuniform in thickness, spikes, referred to as “glitches”, are observed in the data. Such features are intrinsic to data collected using crystal monochromators. We have recently developed a model to show why such features, persist in ratioed data. Here we test the predictions for linearly tapered samples. Our results suggest that the glitch amplitude can be significantly reduced by taking a second spectrum with the sample inverted, and then averaging the two spectra.

### 1. Introduction

Double crystal monochromators, used to obtain high energy resolution for synchrotron X-ray sources, have the undesirable feature that over certain small energy ranges, the flux changes rapidly both in intensity and in spatial distribution [1], as a result of multiple reflections [2–4]. These effects are usually called “crystal glitches”. In EXAFS measurements, over an energy range which includes one or more of the “crystal glitches”, unwanted features also occur in the EXAFS spectra which we have previously called “EXAFS glitches”. They persist in ratioed data (the ratio of the incident flux,  $I_0$ , to the transmitted flux,  $I_t$ ) even when perfectly linear detectors are used and extreme care is taken to minimize higher harmonics; they are intrinsic to data collected using crystal monochromators.

We have recently developed a model [1] which explains why glitches do not ratio out when there is some nonuniformity in the sample. This arises from an energy-dependent change in the spatial distribution of the flux across the slit. If the flux is higher at the thick part of the sample, the effective average thickness will be higher; conversely, if the flux is higher at the thin part of the sample, the sample will appear thinner on average. The quantity measured in EXAFS experiments is  $e^{\mu \bar{l}}$  where  $\mu$  is the absorptance, and  $\bar{l}$  is the effective sample thickness. Clearly a change in the spatial distribution of the flux with energy which results in a variation in  $\bar{l}$  will produce a change in  $e^{\mu \bar{l}}$  (when  $\mu$  is constant). Thus spatial flux variations are

not eliminated in ratioed data. A related model was proposed by Comin et al. [5] to show how glitches arise if the  $I_t$  chamber or the sample is partially shadowed. They used a very narrow, square-well dip in the incident beam profile to model the crystal glitch. This model, applied to a linearly tapered sample, yields a qualitative description of a glitch. However, the shape they assume for the beam profile is not realistic.

The simple model we developed made some specific predictions about a glitch when the thickness of the sample varies linearly across the slit. In this paper we present a study of two glitches using linear tapers of aluminum and Plexiglas to check some of these predictions.

### 2. Vertical beam profiles

We selected two glitches, observed in data taken with Si(2 2 0) crystals (set 8) at SSRL on beamline 4-1, for further study. The first step was to determine the output beam profile for several values of the energy in the vicinity of each glitch. The monochromator entrance slits were opened to 5–6 mm and a scan was made across the entire output beam, using a 0.2 mm vertical slit for each energy. In fig. 1a we show the complicated beam profile observed for a range of energies from 6765 to 6771 eV. Here we plot the flux through a 0.2 mm slit as a function of vertical table position  $y$  and energy  $E$ . A prominent feature clearly moves across the beam profile as the energy is in-

creased. This feature, a dip in amplitude (the dip is near 52 mm for the profile at 6769 eV) followed by an increase in amplitude, is the result of multiple scattering and interferences effects within the monochromator crystals. To see the changes in the profile more clearly, we have plotted in fig. 1b, the difference in amplitude relative to the profile taken at  $E = 6765$  eV. For 1–2 mm high slits, symmetrically positioned at the central position indicated by the vertical dotted line [6], a significant variation in the distribution of the flux across the slit occurs as the energy is increased. For this case, the X-ray beam had significant harmonic contamination that could not be eliminated by detuning. Consequently we expect that a component of the glitch at this energy arises from the presence of harmonics.

Similar, but less detailed data were collected at a second glitch for energies from 9976 to 9980 eV. (see fig. 2a). Here the multi-diffraction features are smaller, and the harmonic contamination is very small. In addition,

other unexpected structure in the beam profile is also observed which does not change with energy. It is a reproducible fine structure on each of the traces in fig. 2a and is *not* noise. In the difference profiles shown in fig. 2b, this fine structure is nearly eliminated and the shift of the narrow multi-diffraction dip with energy is clearly observed. Similar fine structure exists in fig. 1a but is not as obvious in the 3D perspective. We comment more on the fine structure in section 5.

### 3. Glitch shape and amplitude for a wedge-shaped sample: model predictions

Multiple diffractions in the Si(2 2 0) crystals result in a decrease or increase in the output beam intensity as a function of energy. However, this variation in intensity is not uniform across the beam for a particular energy; a dip in the spatial beam intensity profile is present which shifts to higher table positions as the

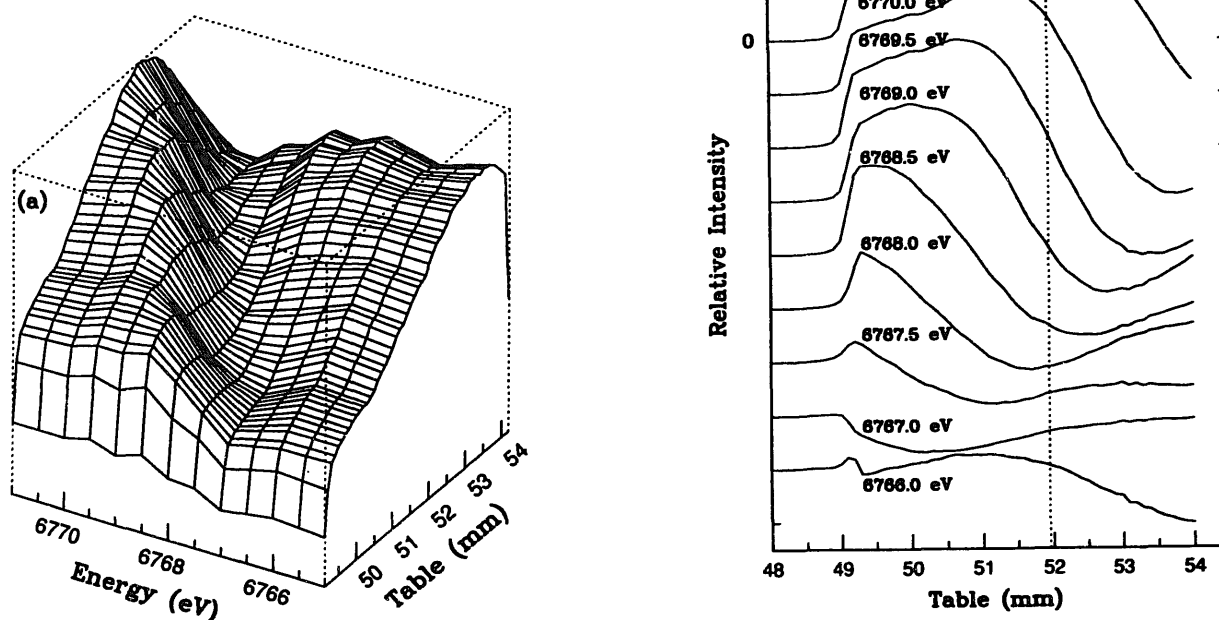


Fig. 1. (a) Incident beam intensity from the monochromator as a function of photon energy and vertical table position for a glitch near 6768 eV. The vertical monochromator entrance slit is 5 mm and the detector slit is 0.2 mm high. The table position is stepped vertically to obtain a profile for a given energy. Points in each profile at the same table position are connected by lines. A multiple diffraction feature moves across the profile between 6766 and 6770 eV. Maximum amplitude (top of cube defined by dotted lines) is 1.95. (b) The incident beam intensity distribution relative to the profile taken at  $E = 6765$  eV. The dotted line indicates the central position of the slit for the data presented in fig. 5. The scale is expanded as indicated.

energy is increased as shown in figs. 1 and 2. Consequently, the spatial distribution of the flux within the slits changes considerably with energy.

The model presented earlier [1] made the following predictions for a glitch, assuming for simplicity that the multi-diffraction feature in the beam profile could be described by a symmetric dip, with a width that was roughly  $\frac{1}{2}$  that of the beam profile. The present data (figs. 1 and 2) show that the spatial intensity variation is not symmetric and that the width of the feature can vary considerably ( $\sim 2$  mm in fig. 1 and  $\sim 0.7$  mm in fig. 2).

1) The glitch would have both positive and negative lobes; the two lobes would be of equal height for a symmetric dip, but of unequal heights for a more realistic asymmetric spatial flux variation.

2) The sign of the glitch (i.e., whether it first increases or first decreases) changes when a wedge shaped sample is inverted. Consequently, if one adds together the two spectra for a sample with the wedge up and for the wedge down, the glitch amplitude should cancel if the same part of the wedge remains in the X-ray beam.

3) The magnitude of the glitch depends on the slit height. We define the slit opening as the region  $-a/2 \leq y \leq a/2$ . (Total slit height =  $a$ ). In a linearized ap-

proximation, for which both the sample thickness,  $t$ , and the incident flux,  $F(y, E)$  (units: photons/s mm), vary linearly with  $y$ , the glitch amplitude then varies as  $a^2$ . From the data presented in figs. 1 and 2, a linear approximation for  $F(y, E)$  is not a good approximation for  $a \geq 1$  mm.

For a quantitative comparison, we have used the known thickness of the wedge,  $t(y)$ , and the measured spatial dependence of the beam,  $F(y, E)$ , to calculate the glitch shape for several different slit openings. We define the incident,  $I_0$ , and transmitted,  $I_t$ , beam intensities by the equations:

$$I_0(E) = \int_{-a/2}^{a/2} F(y, E) dy, \tag{1}$$

$$I_t(E) = \int_{-a/2}^{a/2} F(y, E) e^{-\mu t(y)} dy, \tag{2}$$

where  $\mu$  is the sample absorptance. We then define the ratio,  $R(E)$ , by

$$R(E) = I_0(E)/I_t(E). \tag{3}$$

This definition applies both to experimental values of  $R(E)$  as well as to the quantity calculated using eqs. (1) and (2).

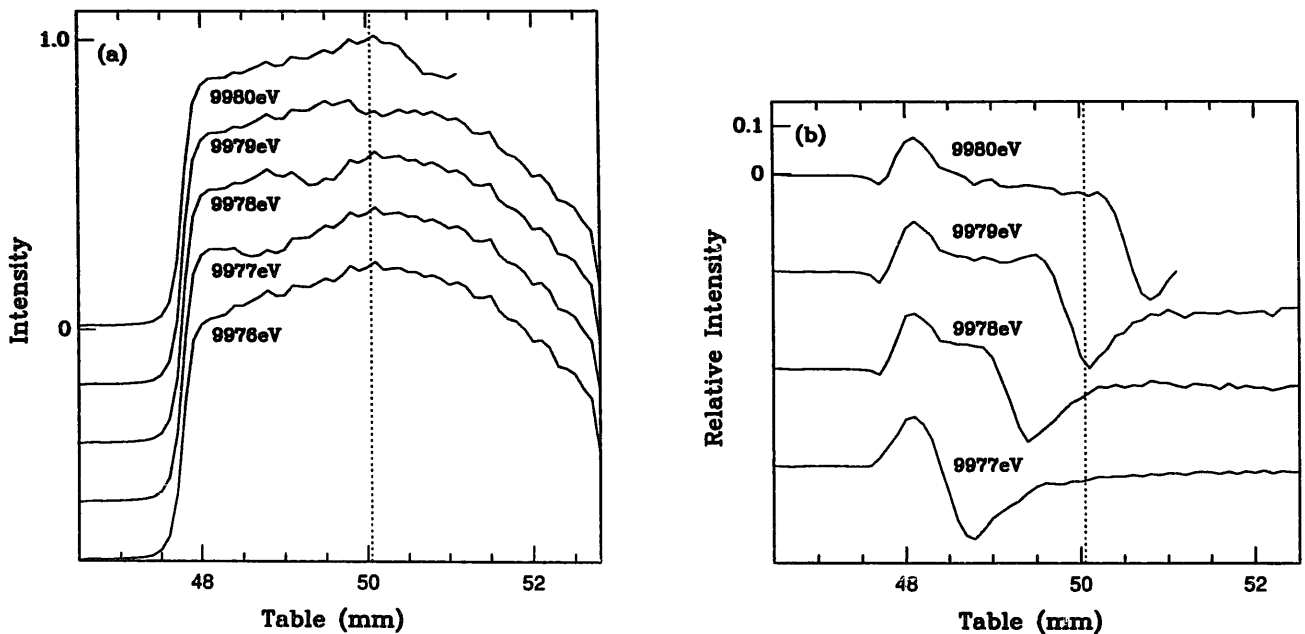


Fig. 2. (a) The incident beam intensity from the monochromator as a function of photon energy and vertical table position for a glitch near 9978 eV. The monochromator entrance slit is 5 mm, and the slit for the detector is 0.2 mm. (b) The incident beam intensity relative to the profile taken at 9976 eV. In this case the multiple diffraction feature is very narrow. The dotted line indicates the central position of the slit for the data presented in fig. 3. Note that most of the spatial, energy-independent structure observed in fig. 2a is removed, indicating that this structure is reproducible and time independent over times of order 15 min.

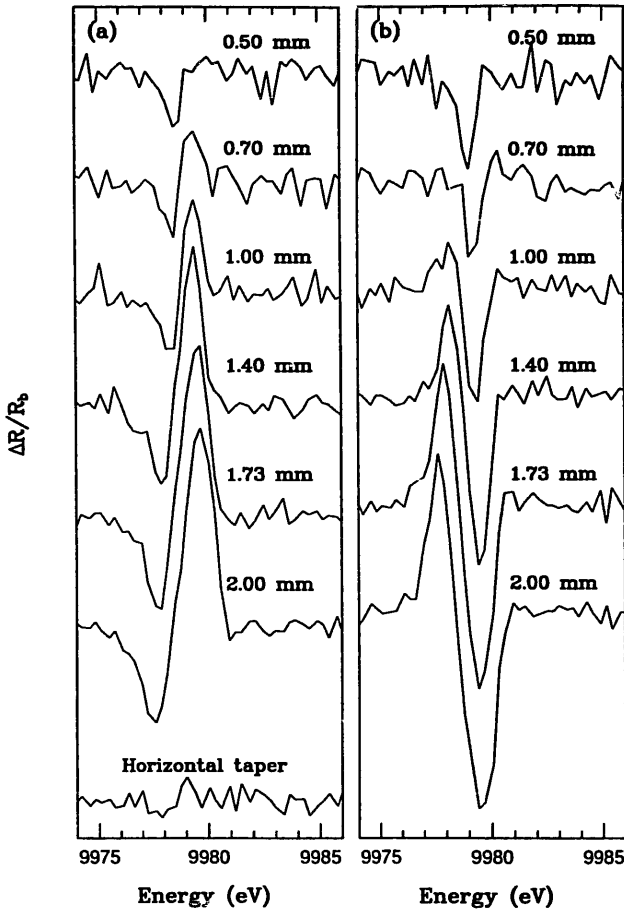


Fig. 3. A plot of the normalized glitch,  $\Delta R/R_b$ , for various vertical slit heights,  $a$ , for the tapered aluminum sample. (a) The thin end of the wedge is up. The bottom trace in (a) was collected with the sample turned  $90^\circ$  so that the taper was horizontal. (b) A plot of  $\Delta R/R_b$  with the sample inverted (thin end of the wedge is down).

4. Data

We collected data in the standard transmission mode for a small energy range about each of these glitches, using 0.3 eV steps in energy. For the lower energy glitch at 6768 eV, we used a Plexiglas taper, while for the second glitch (at 9978 eV), we used an aluminum taper. Scans were taken with the taper removed to ensure that the sample mount and the detectors did not contribute. For the aluminum taper, the average sample thickness,  $\bar{t}$ , is 0.38 mm and the variation of  $t$  with  $y$  (in mm) has the form

$$t = \bar{t} + \alpha y; \quad \text{with } \alpha = 0.05. \quad (4)$$

For the Plexiglas sample, the wedge is not quite a linear taper (the center is about 20% too thin). For this sample  $t(y)$  is approximately given by ( $\bar{t}' = 1.5$  mm)

$$t(y) = \bar{t}' + \alpha' y; \quad \text{with } \alpha' = 0.2. \quad (5)$$

In fig. 3a we show energy sweeps for a series of slit heights,  $a$ , with the thin side of the aluminum wedge up (defined as wedge up). We calculate a background function,  $R_b(E)$ , from a straight line fit to the ratioed data above and below the glitch. The quantity plotted in fig. 3a is the fractional relative change in the experimental values of  $R(E)$  relative to  $R_b(E)$ , i.e.,

$$\frac{\Delta R}{R_b} = \frac{R(E) - R_b(E)}{R_b(E)}. \quad (6)$$

The glitch clearly has both a positive and a negative lobe, as predicted, and increases significantly in peak-to-peak amplitude as the slit height is increased. The amplitude increase is not as fast as the  $a^2$  dependence predicted, and becomes weaker at large  $a$ . To check

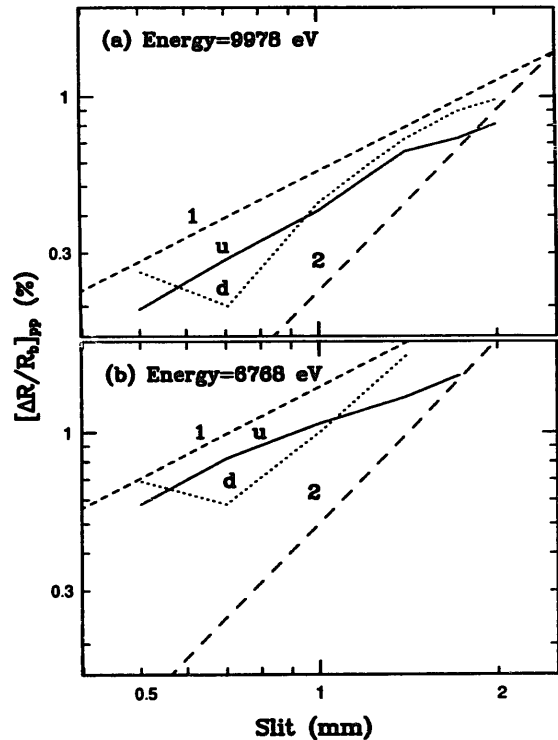


Fig. 4. A plot of the peak-to-peak glitch amplitude,  $(\Delta R/R_b)_{pp}$ , on a log-log scale as a function of the slit height,  $a$ , for the 9978 eV feature in (a) (see fig. 3) and the 6768 eV feature in (b) (see fig. 5). u is wedge up and d is wedge down. The dashed lines labeled, 1 and 2, correspond to linear and quadratic dependencies on the slit height,  $a$ .

the power law behavior, we have plotted our limited data (see fig. 4a) on a log-log scale as a function of  $a$  and included straight lines, corresponding to linear and quadratic dependencies, for comparison.

In fig. 3b we show the corresponding data with the wedge inverted. The glitch is also inverted as predicted and has a similar change in amplitude as the slit height is increased. The glitch amplitude dependence on  $a$  is also plotted in fig. 4a for this orientation of the wedge.

The last trace in fig. 3a shows a sweep with the wedge turned horizontally. Now the sample is uniform in the vertical direction but varies in thickness from 0.25 mm to 0.5 mm along the 5 mm wide slit. No evidence for a glitch is observed. This suggests that, at least for this feature, there is little change in the

spatial distribution of the beam in the horizontal direction over the energy range of the glitch.

In fig. 5a and 5b we plot similar data,  $\Delta R/R_b$ , obtained using the plexiglass wedge sample for the glitch at 6768 eV. (wedge up (fig. 5a) and wedge down (fig. 5b)). Again the glitch is inverted when the wedge is inverted but this time the shape is not quite the same, in part because the wedge is not quite linear (slightly concave). The amplitude of the glitch does increase as the slit height increases and in fig. 4b we plot the peak-to-peak glitch height as a function of  $a$  on a log-log scale. The amplitude increase with  $a$  is quite similar to that observed for the 9978 eV glitch.

A point to note for both figs. 3 and 5 is that most of the glitch occurs over a very narrow energy range,  $\leq 7$  eV for both cases. Consequently at energies just above an absorption edge, the glitch will contribute to several points of a typical EXAFS spectrum, while for high  $k$ , only a single point may be affected as the energy step size for  $\Delta k = 0.05 \text{ \AA}^{-1}$ , is  $\sim 6$  eV at  $k = 15 \text{ \AA}^{-1}$ .

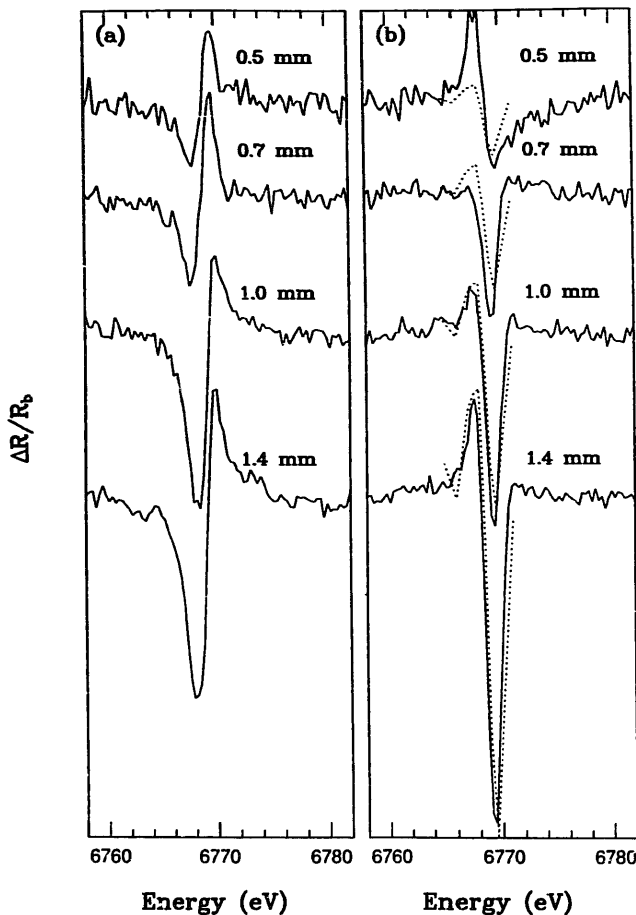


Fig. 5. A plot of the normalized glitch,  $\Delta R/R_b$ , for various vertical slit heights  $a$ , for a Plexiglas sample. For (a) the thin end of the wedge is up while in (b) the thin end is down. For this energy range, there is some contribution from harmonics. The dotted lines show the simulation results.

## 5. Comparisons and discussion

### 5.1. Glitch inversion

The linearized model predicts that when a wedge-shaped sample is inverted, the glitch is also inverted with no change in shape. To test this prediction we first superimposed the two traces for the glitch near 9978 eV for which the slit height is 2 mm (see traces in figs. 3a and 3b). In fig. 6 these two traces are replotted, with the trace from fig. 3a inverted. The agreement for the large lobe is excellent, but there is a small disagreement on the smaller lobe. To compare the size of the discrepancy with the level of the noise in the spectra, we plot the normalized sums of the traces for each slit size in fig. 6b. The cancellation of the glitch is remarkable although not quite complete, and the amplitude of the remaining glitch is about twice the peak-to-peak noise amplitude in the original data (see noise level in fig. 6a). A slight shift in energy of one of the peaks can improve the cancellation slightly (see fig. 6b).

The precise source of the remaining small glitch is not clear; in part it must arise from the sample position. It is unlikely that when the wedge was inverted, exactly the same piece of the sample was in the beam. We estimate this uncertainty to be  $\pm 0.1$  mm. However it is probably an intrinsic aspects of glitches produced as described above. Only in the linearized model will the sum of glitches for a wedge up and a wedge down sample, exactly cancel. If one expands functions in eq. (2) to higher order and includes terms of order  $\alpha^2$  ( $\alpha$  is the slope of the thickness variation defined by eq. (4))

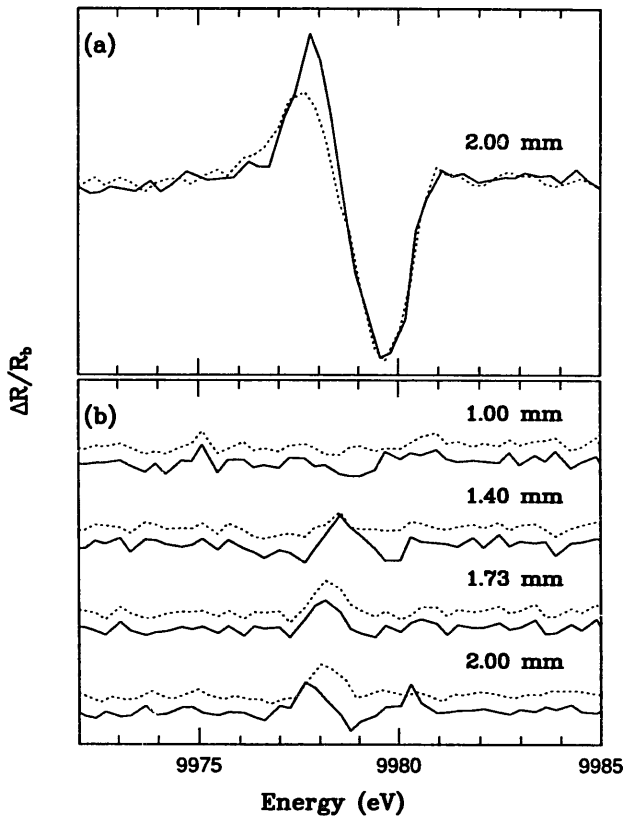


Fig. 6. (a) A comparison of the traces for the 9978 eV glitch observed using 2.00 mm output slits. The trace from fig. 3a is inverted and shifted by 0.14 eV to show that the glitches have the same shape and that the difference between figs. 3a and 3b is primarily an inversion. In (b) we have averaged the corresponding traces from figs. 3a and 3b for the same slit heights without an energy shift (solid lines) and with a small energy shift (dotted lines). The vertical scale is the same as in (a) above. The glitch cancels out very well.

a term proportional to  $\alpha^2$  does not cancel out. The remaining glitch might also arise in part from a small amount of harmonic contamination, from small energy drifts of the monochromator as a result of motion of the electron beam or from a change in temperature of the monochromator crystals. The important point to note, however, is that to first order the glitch is inverted when the wedge sample is inverted and that the cancellation in the sum is close to complete. This suggests a procedure for significantly reducing the glitch amplitude in EXAFS spectra. After collecting an EXAFS spectrum, the sample is inverted and a second spectrum collected. The average of these two spectra should be nearly glitch free. We note that this procedure is particularly important in the low  $k$  range of EXAFS data as it is often impossible to separate a

glitch from the EXAFS oscillations over this range. Another means of averaging would be to flip the sample and collect two data points at each energy, one of them with the sample inverted [7]. This would minimize drift effects but would be somewhat more complicated for low temperature measurements.

For the glitch near 6768 eV, the situation is different. A review of fig. 5 shows that there is a significant change in shape when the sample is inverted. In fig. 7 we again plot the normalized sum of the two traces for the same slit height. In this case, there is a well defined remaining glitch that does not cancel, and does not have both a negative and positive lobe. We suggest that this is probably a combined result of the presence of harmonics, a slight curvature of one surface of the plexiglass sample, and errors in positioning the sample upon inversion.

What are the implications for real EXAFS experiments? First, most samples are not simple linear tapers, but have random variations across the slit (they also have pinholes which we will address in a separate paper). To the extent that we might model a real sample as a series of short tapers with both positive and negative values of  $\alpha$  ( $\alpha = dt/dy$ ), then there may be some averaging within the sample itself. Second, the sample inversion should be done about a line through the center of the slit. Random sample variations plus errors in positioning the inverted sample probably will decrease the amount of glitch suppression in a simple average. However, a weighted average may be possible if the glitch shapes are similar but the amplitudes are different in the data for the non-inverted and inverted geometries.

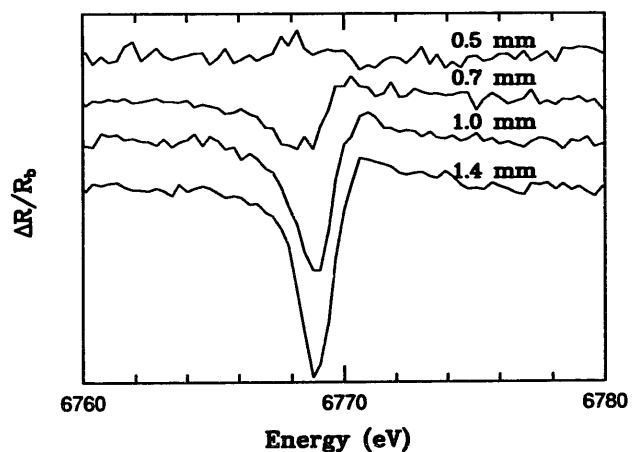


Fig. 7. The average of the corresponding traces from figs. 5a and 5b. There is a considerable decrease in the amplitude of the resultant glitch, but because of complications possibly arising from harmonic contamination and from curvature in the Plexiglas sample, the cancellation is not complete.

### 5.2. Glitch shape

Given the shape of the beam profile  $F(y, E)$  as a function of position and energy and the thickness of the sample as a function of position  $t(y)$ , we can calculate  $R(E)$  from eq. (3). However many beam profiles are needed for a reasonable calculation. We unfortunately do not have enough data to estimate the glitch shape for the 9978 eV glitch. Enough profiles do exist for a crude estimate of the 6768 eV glitch but because of the complications of a slightly nonlinear sample thickness and some harmonic contamination, a quantitative comparison is not easily made. However qualitatively, the calculated glitch shape using the data of fig. 1a has a very similar shape to that observed experimentally in fig. 5b, as shown by the dotted line in fig. 5b.

### 5.3. Additional fine structure

Lastly we return to the nearly energy-independent fine structure that is on the beam profile (see fig. 2a). We have observed similar structure on profiles at other energies and also on profiles obtained using Si(1 1 1) monochromator crystals. The magnitude of the structure is roughly 2% when a 200  $\mu\text{m}$  slit is used for the spatial measurements. This structure appears to be reasonably stable on the scale of 200  $\mu\text{m}$  for data collected at one point every two seconds. The positions of the small steps do not change with energy or with time over the 15–20 min required to collect the data in fig. 2a. However, a close review of fig. 2b shows that the amplitude of the structure does change with energy (or perhaps with time since the profiles were collected sequentially). Some time dependence of the position and amplitude is expected because of fluctuations in the beam position.

The presence of this structure has two important implications when it is present within the monochromator exit slits in an EXAFS experiment. First consider amplitude variations with energy. Then for nonuniform samples these intensity variation will not be eliminated in ratioed data; it is like the glitch problem but on a smaller scale. This will produce noise and possible lead to slowly varying fluctuations in the background of the EXAFS oscillations. Second, if the position of the structure is slightly time dependent and moves up and down within the slits (by 50  $\mu\text{m}$  for example) additional noise will be generated. Our rough estimates of these contributions to the noise are in the range  $10^{-4}$  to  $5 \times 10^{-4}$ , very comparable to the S/N in our best data. This structure in the beam (coupled with sample inhomogeneities) may set the noise level in EXAFS experiments, at a value much higher than

expected from the number of photons collected (typically  $> 10^{10}/\text{s}$  on a wiggler beam line).

The source of the fine structure is unknown at present. These features may arise from variations in the reflectivity of the monochromator crystals as the energy is changed, possibly as a result of surface thermal gradients. They might also be produced by X-ray beam optics problems (i.e. a part of the beam has a glancing reflection at a window or other optical element and passes through part of the monochromator). More speculatively, there may be structure in the X-ray beam itself. Clearly the fine structure deserves further attention.

## 6. Conclusion

We have shown that the simple model recently developed describes the glitches in ratioed data quite well for a linearly tapered sample. The shape and size of a glitch is determined by the slit opening and by the change in the spatial distribution of flux across the slit as the energy is changed. No glitch is observed when the wedge is removed or when the wedge is horizontal (for the small range of energies considered here.) The beam profile also shows considerable fine structure as a function of position which may well contribute to noise in the EXAFS spectra if it varies with energy or in time as a result of electron beam motion. Further experiments on beam profiles are planned.

## Acknowledgement

We thank George Brown and J. Boyce for helpful discussions. The experiments were performed at SSRL, which is funded by the Department of Energy under contract DE-AC03-82ER-13000, Office of Basic Energy Sciences, Division of Chemical Sciences, and the National Institute of Health, Biotechnology Resource Program, Division of Research Resources. The work is supported in part by NSF grant number DMR-90-04325.

## References

- [1] F. Bridges and X. Wang, Nucl. Instr. and Meth. A307 (1991) 316.
- [2] Z.U. Rek, G.S. Brown and T. Troxel, EXAFS and Near Edge Structure III, eds. K.O. Hodgson, B. Hedman and J.E. Penner-Hahn (Springer) Proc. in Phys. 2 (1984) p. 511.

- [3] K.R. Bauchspiess and E.D. Crozier, *ibid*, p. 514.
- [4] G. Van Der Lann and B.T. Thole, *Nuc. Instr. and Meth. A263* (1988) 515.
- [5] F. Comin, L. Incoccia and S. Mobilio, *J. Phys. E 16* (1983) 83.
- [6] The slits were initially centered below the Mn k-edge. The data presented in fig. 1 all have a component of a glitch present. Consequently, the slits do not appear to be centered on the beam.
- [7] Suggested by W. Warburton, private communication.